Biochemical and Biophysical Research Communications 417 (2012) 576–581

Contents lists available at SciVerse ScienceDirect

Biochemical and Biophysical Research Communications

journal homepage: www.elsevier.com/locate/ybbrc

Investigation of a potential mechanism for the inhibition of *Sm*TGR by Auranofin and its implications for *Plasmodium falciparum* inhibition

Antonia Caroli [a,1], Silvia Simeoni [a,1], Rosalba Lepore [a], Anna Tramontano [a,b,*], Allegra Via [a,*]

[a] Department of Physics, Sapienza University of Rome, Rome, Italy
[b] Istituto Pasteur Fondazione Cenci Bolognetti, Sapienza University of Rome, Rome, Italy

ARTICLE INFO

Article history:
Received 24 November 2011
Available online 8 December 2011

Keywords:
S. mansoni
P. falciparum
Thioredoxin Glutathione Reductase
Auranofin

ABSTRACT

Schistosoma mansoni and *Plasmodium falciparum* are pathogen parasites that spend part of their lives in the blood stream of the human host and are therefore heavily exposed to fluxes of toxic reactive oxygen species (ROS). *Sm*TGR, an essential enzyme of the *S. mansoni* ROS detoxification machinery, is known to be inhibited by Auranofin although the inhibition mechanism has not been completely clarified. Auranofin also kills *P. falciparum*, even if its molecular targets are unknown. Here, we used computational and docking techniques to investigate the molecular mechanism of interaction between *Sm*TGR and Auranofin. Furthermore, we took advantage of the homology relationship and of docking studies to assess if *Pf*TR, the *Sm*TGR malaria parasite homologue, can be a putative target for Auranofin. Our findings support a recently hypothesized molecular mechanism of inhibition for *Sm*TGR and suggest that *Pf*TR is indeed a possible and attractive drug target in *P. falciparum*.

1. Introduction

Parasites that spend part of their lives in the blood stream are heavily exposed to fluxes of toxic reactive oxygen species (ROS). Two such examples are *Schistosoma mansoni* and *Plasmodium falciparum*, the etiological agents of schistosomiasis and malaria. To maintain the redox balance necessary to survive, these parasites have evolved specialized ROS detoxification machineries, the enzymes of which are essential and therefore promising targets for the development of new drugs.

S. mansoni has a complex life cycle involving two hosts, a snail and a human one. Praziquantel is currently the only drug used to treat the disease and its consistent use is causing concern about the appearance of drug resistance. The life cycle of *P. falciparum* also involves two hosts, a mosquito and a human one. Malaria is mainly treated with the fast-acting and inexpensive chloroquine associated with antifolate drugs [1]. The continued use of these compounds has increased the appearance of drug-resistance around the world. Today, the most effective class of antimalarial drugs is represented by artemisinin derivatives, the effectiveness of which is increasingly compromised by the appearance of *P. falciparum* strains showing a reduced clinical response to artemisinin-containing drug combinations [2].

Owing to the intrinsic difficulties of developing new antimicrobial agents [3], no new classes of drugs against the two parasites have been recently introduced into the clinical practice. The identification of new drug targets, on one hand, and of novel molecules active on the parasites, on the other, is urgently needed.

We started from the observation that both parasites are heavily exposed to ROS fluxes in the blood stream and focused our attention on homologous enzymes belonging to the parasite detoxification machinery, with the aim of detecting new potential drug targets.

Recently, a Thioredoxin Glutathione Reductase (*Sm*TGR) has been identified as a key enzyme in the detoxification pathway of *S. mansoni*. *Sm*TGR shuttles electrons from NADPH to Thioredoxin (Trx) and to Glutathione (GSSG). It is a homodimeric selenoprotein, with each monomer consisting of a unique fusion between a Glutaredoxin (Grx) domain (residues 1–106) and a Thioredoxin Reductase (TR) domain (residues 107–598) [4], which contains a selenocysteine (Sec597) as the penultimate C-terminal amino acid [5]. Each monomer has a large cleft occupied by FAD and contains 15 cysteines (Cys), three belonging to the Grx domain and 12 to the TR domain. At least six cysteines are conserved in pairs and are known to change their oxidation state during the catalytic activity [5]: in the TR domain, Cys154 and Cys159 are close to FAD and Cys596 and Sec597 are at the C-terminus, whereas Cys28 and Cys31 belong to the Grx domain. Cys520 and Cys574 form a further pair that is potentially redox active.

A reasonable hypothesis that has been proposed for the enzyme redox mechanism is that electrons are transferred first from NADPH to the primary redox center of the enzyme, which is formed by FAD and by the Cys154–Cys159 pair, and, subsequently,

* Corresponding authors. Address: Department of Physics, Sapienza University of Rome, P.le Aldo Moro 5, 00185 Rome, Italy. Fax: +39 064440062.
E-mail addresses: anna.tramontano@uniroma1.it (A. Tramontano), allegra.via@uniroma1.it (A. via).
[1] These authors contributed equally to this work.

0006-291X/$ - see front matter © 2011 Elsevier Inc. All rights reserved.
doi:10.1016/j.bbrc.2011.12.009

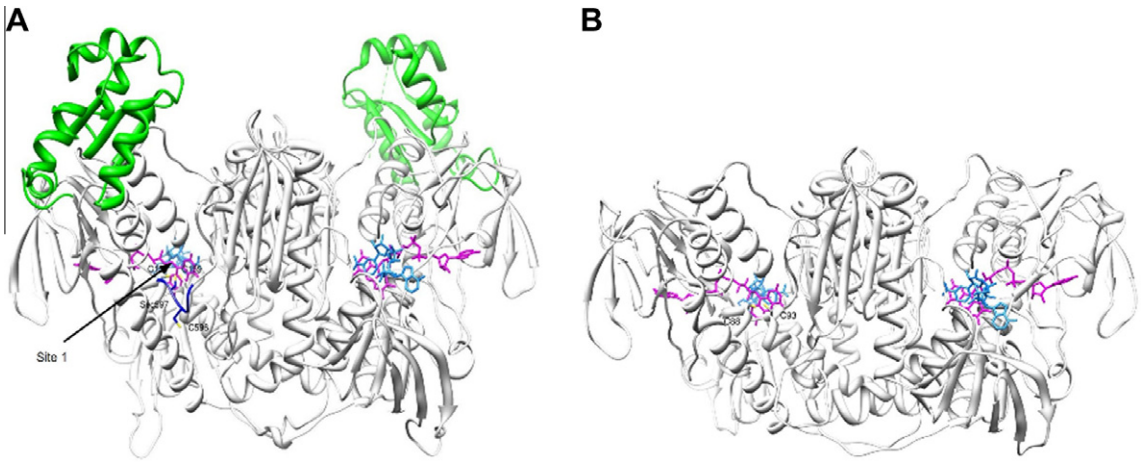

Fig. 1. The structures of full-length *Sm*TGR and *Pf*TR. (A) *Sm*TGRfl structure: the C-terminus is in blue; the Grx domain in green; the TR domain in white; the FAD in magenta; the NADPH in light blue; Site 1 cysteines (Cys154 and Cys159), Sec597, and Cys596 are labeled. (B) *Pf*TR structure: the FAD is in magenta; the NADPH light blue; Site 1 cysteines (Cys88 and Cys93) are labeled. (For interpretation of the references to color in this figure legend, the reader is referred to the web version of this article.)

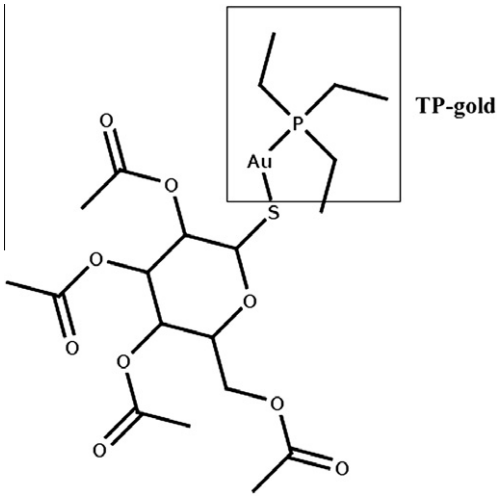

Fig. 2. Auranofin (AF) and triethylphosphine-gold (TP-gold) chemical structures.

to the C-terminal Sec597. The reduced Sec597 can then transfer the electrons either directly to Trx or to GSSG via the Grx domain Cys28-Cys31 pair [6].

In *Plasmodium*, as well as in human, two distinct enzymes, a Thioredoxin Reductase (*Pf*TR), homologous to *Sm*TGR, and a Glutathione Reductase (*Pf*GR), fulfill the same function as *Sm*TGR in *Schistosoma*. *Pf*TR, which, similarly to *Sm*TGR, is a homodimeric flavo-protein, also contains two TR domains and the catalytic site is very well conserved across the TR family. At the C-terminal, though, the Cys-Gly-Gly-Gly-Lys-Cys sequence replaces the *Sm*TGR Cys-Sec-Gly sequence. The Grx domains are absent in *Pf*TR. *Pf*TR knock-out studies show that the enzyme is essential for the survival of the erythrocytic stages of the parasite [7].

Recent studies have identified Auranofin (AF) (Fig. 2), a gold compound in clinical use as anti-arthritic, as a promising *Sm*TGR inhibitor [4]. AF has also been shown to inhibit the growth of *P. falciparum* [8], even though its molecular targets are still unknown. The molecule is a pro-drug that delivers gold to a number of target proteins [9], has a linear, two-coordinated Au(I) center with a triethylphosphine-gold (TP-gold) ligand and a tetraacetylthioglucose ligand. The phosphine moiety confers membrane solubility to AF, whereas the tetraacetylthioglucose ligand is excreted *in vivo*, suggesting that the TP-gold is the active therapeutic agent [10]. AF inhibits *Sm*TGR at nanomolar concentration (IC_{50} = 7 nM) and substantially reduces worm burden in mice [4].

Six *Sm*TGR structures are currently available in the Protein Data Bank [11]: five are high resolution structures (between 1.90 and 2.55 Å) lacking the two last residues at the C-terminus, Sec597 and Gly598, and one is a medium-resolution structure (3.10 Å) of the full-length protein, *Sm*TGRfl (Table 1). Angelucci et al. determined the co-crystal of *Sm*TGR with gold atoms at 2.55 Å resolution [12]. In this work, the authors incubated the protein with AF in both its truncated (3 μM of *Sm*TGR and 8 μM of AF) and full-length (20 nM of *Sm*TGRfl and 50 nM of AF) forms. In the former case, the crystal structure obtained after the incubation only showed the presence of gold atoms (and not the entire compound) bound at three different sites of the enzyme, none of them directly involving the C-terminal Sec residue. In the truncated *Sm*TGR, the kinetics of inhibition by AF is 200-fold slower than in the full-length variant (inactivation rate constant = 0.21 min^{-1}), but it is accelerated by the addition of benzene selenol (BzSe), suggesting that Sec597 may play an important role in accelerating the inhibition of *Sm*TGR.

These results indicate that the AF molecule is able to transfer the gold atom to *Sm*TGR *in vitro*, at least when it is present in excess, whereas the inhibitory action is likely to be performed by TP-gold *in vivo*. In both cases, there are at least two open questions: Does the transfer of the gold atom by the inhibitors require binding of the donors to the enzyme or is a transient interaction sufficient? Is the gold atom directly transferred to the three sites or does the C-terminal Sec mediate the transfer of gold from the compound to the redox-active cysteine pair of *Sm*TGR, as proposed by Angelucci et al. [12]? Furthermore, the biological relevance of the three sites, given the stoichiometry of gold versus protein in the experiment, is not obvious. One possible way to answer these questions is to assess, taking advantage of docking experiments, whether there exist binding sites for AF and/or TP-gold and, if so, where are they located. Moreover, since AF also inhibits the growth of *P. falciparum* [8] but its molecular targets are still unknown, we used our findings on *Sm*TGR and the observation that both *S. mansoni* and *P. falciparum* are heavily exposed to fluxes of toxic ROS, to assess the likelihood that *Pf*TR, the homologue of *Sm*TGR in *Plasmodium*, is the target of AF and/or of its TP-gold derivative. Our results are obtained through computational studies, but are also based on previous structural and biochemical data on the enzymes [5,6,12], which increases our confidence in the conclusions.

Table 1
List of the *Sm*TGR structures deposited in the PDB.

PDB code	C-term tail variant	Form	Complexed with	Resolution (Å)	Ref.
2V6O	Truncated	Reduced	FAD	2.20	[5]
3H4K	Truncated	Reduced	FAD, gold	2.55	[12]
2X8G	Truncated	Oxidized	FAD	1.90	[6]
2X99	Truncated	Oxidized	FAD, NADPH	2.30	[6]
2X8H	Truncated	Oxidized	FAD, GSH	1.90	[6]
2X8C	Full-length	Reduced	FAD	3.10	[6]

2. Materials and methods

2.1. Homology modeling

The amino acid sequence of the Thioredoxin Reductase from *P. falciparum* (*Pf*TR) is 541 amino acid long (UniProt Accession: Q25861). The search for templates was performed using the HHpred software (http://toolkit.tuebingen.mpg.de/hhpred) against the PDB database [11].

The best templates selected are *Mus musculus* TR (*Mm*TR, PDB: 3DGZ), *Homo sapiens* TR (*Hs*TR, PDB: 2ZZC) and *Sm*TGR (PDB: 2V6O) with 48%, 46% and 48% sequence identity with the *Pf*TR sequence, respectively. The *E*-value is lower than 5.6×10^{-4} for all templates.

We used the MODELLER software [13] to build the *Pf*TR model in its homodimeric form with the FAD cofactor. The N-term and C-term tails, 35 and 9 residue long, respectively, were not modeled because they were absent in the available templates. As for the modeling of the insertion between the target residues 441 and 453 (Fig. S1, Supplementary material), we generated 20 loop conformations with the *loopmodel* tool of MODELLER. The best loop model was chosen based on the DOPE statistical potential score. Fifty models were built and the final model, selected on the basis of the MODELLER objective function, was evaluated using both the ProQ model quality assessment program [14] and the MetaMQAP server [15].

2.2. Docking procedures

2.2.1. Ligand and protein preparation

The three-dimensional structure of the TP-gold moiety was obtained using the ChemAxon Marvin 5.5.0.1 software (http://www.chemaxon.com). The Auranofin crystal structure was retrieved from the Cambridge Structure Database (CSD) (http://www.ccdc.cam.ac.uk). The semiempirical calculation of ligand partial charges was performed using the PM6 method by MOPAC2009 (http://OpenMOPAC.net/). The resulting charges were used in all docking calculations. The *Sm*TGR atom coordinates (Table 1) were obtained from the Protein Data Bank. The *Pf*TR structure was obtained by homology modeling (see Section 2 above). The hydrogen atoms were added to *Sm*TGR and *Pf*TR using the xLeap Amber module (http://ambermd.org/#AmberTools). The NADPH cofactor coordinates were obtained by superimposing the mouse Thioredoxin Reductase-NADPH (PDB: 1ZDL) complex to the structure of *Sm*TGRfl and *Pf*TR. To relieve hydrogen unfavorable steric contacts, the protein structures were minimized by steepest descent procedure (1000 iterations) followed by conjugate gradient (5000 iterations) in explicit solvent with the Amber package. All the heavy atoms of the proteins were kept fixed during the simulation.

2.2.2. Molecular docking

The procedure used to identify the ligand preferential binding sites in the enzyme structures consisted of two steps: (i) "blind docking", i.e. coarse grained unbiased search for putative binding sites on the whole protein surface; (ii) "local docking", where the sites selected in the first step were searched more finely to find the most favorable orientations in the sites.

Docking experiments were performed using Autodock 4.2 [16]. In blind docking experiments, a $230 \times 196 \times 196$ grid point box, enclosing the entire protein structure, with a grid spacing of 0.55 Å centered on the protein center of mass was used. Given the relatively large size of the proteins (*Sm*TGR and *Pf*TR are 130 and 120 kDa, respectively), we manually modified some AutoDock scripts (*autogpfCommands.py*) to increase the box size and recompiled the program. Two parameters were specifically set in the Autodock parameter file, namely the sum of Van der Waals radii of two atoms (Rii = 1.60 Å) and the VdW well-depth (epsii = 0.875 kcal/mol). These values were based on Autodock parameter values for transition metals [17].

In local docking experiments, a smaller box ($55 \times 50 \times 45$ grid point with a grid spacing of 0.375 Å) centered on the ligand binding site was used.

In both the blind and local docking experiments, 100 independent Lamarckian genetic algorithm (LGA) runs were performed. Pseudo-Solis and Wets minimization methods were applied using an initial population of 150 randomly placed individuals, a maximum number of 2.5×10^6 energy evaluations, and a maximum number of 2.7×10^4 generations. A mutation rate of 0.02 and a crossover rate of 0.8 were used. Each docking calculation generated 100 different runs.

3. Results

3.1. S. mansoni Thioredoxin Glutathione Reductase (SmTGR)

We used both the truncated and full-length variants of the protein in our docking simulations. For the truncated form we selected 3H4K (without NADPH) and 2X99 (with NADPH), and for the full-length variant we used the only available crystal structure, namely 2X8C, which does not contain NADPH (see Table 1).

3.2. Auranofin

Blind docking experiments of AF into the truncated structure produced several putative binding modes, which, however, did not cluster around any specific site. Moreover, the computed free energy of all the predicted binding modes was larger than 2.5 kcal/mol (Table 2). In particular, no clustering of solutions was found near the catalytic site close to FAD, which lies in a hydrophobic pocket that we call Site 1 in the following (Fig. 1). The analysis of the terms contributing to the binding free energy showed that the highest contribution was due to the AF torsional free energy (+4.12 kcal/mol), suggesting that, in order to enter the catalytic site, AF is forced to assume an unfavorable conformation.

Table 2
Results of the blind docking experiments of AF into *Sm*TGR (truncated and full-length) and *Pf*TR, in presence and absence of NADPH.

Enzyme	NADPH	No. of different clusters/total number of conformations	No. of conformations in the most populated cluster/total number of conformation	Estimated range of binding free energy (min/max) (kcal/mol)
*Sm*TGR	Yes	98/100	2/100	−2.65/+0.28
	No	98/100	2/100	−2.80/+0.04
*Sm*TGRfl	Yes	98/100	2/100	−2.41/+0.92
	No	98/100	2/100	−2.68/+0.09
*Pf*TR	Yes	96/100	2/100	−3.03/+0.04
	No	97/100	2/100	−2.50/+0.15

Table 3
Results of the blind docking experiments of AF into the NADPH site of *Sm*TGR (truncated and full length) and *Pf*TR.

Enzyme	No. of conformations (in each NADPH binding site)/total number of conformations	Estimated binding free energy (kcal/mol)
*Sm*TGR	1/100	−1.7
*Sm*TGRfl	1/100	−1.2
*Pf*TR	1/100	−1.3

Table 4
Results of the blind and local docking experiments of the TP-gold moiety into the *Sm*TGR (truncated and full length) and *Pf*TR catalytic site close to FAD (Site 1).

Enzyme	Docking experiment type	No. of different clusters/total number of conformations	No. of conformations in the most populated cluster/total number of conformation	Estimated binding free energy (kcal/mol) of the best docked conformation
*Sm*TGR	Blind	18/100	15/100	−4.03
	Local	1/100	100/100	−4.02
*Sm*TGRfl	Blind	16/100	13/100	−3.67
	Local	3/100	79/100	−3.73
*Pf*TR	Blind	15/100	19/100	−4.71
	Local	2/100	88/100	−4.71

The same procedure was repeated using *Sm*TGRfl and the results were not much different in terms of solutions in Site 1 and of their computed free energy (Table 2).

One of the gold atoms experimentally detected in the X-ray structure was located at the NADPH binding site [12]. This indicates that AF might have an alternative mechanism of inhibition, which implies competition with NADPH, at least in the experimental conditions of the crystallization experiment. To evaluate the likelihood of this hypothesis, we also performed docking experiments using both *Sm*TGR and *Sm*TGRfl in the absence of NADPH. Once again, the computed binding energies do not support the possibility of favorable binding of AF to *Sm*TGR in either forms (Table 2). In fact, the single AF conformation found in each NADPH binding site has a binding free energy of about −1.7 kcal/mol (Table 3). We therefore favor the hypothesis that the gold atom observed near the NADPH site in the crystal structure reached its site through an indirect mechanism, rather than by direct binding of AF to the protein, and that its presence might be observed only when the concentration of AF in solution is high.

3.3. TP-gold derivative

In contrast with the docking results for AF, the results of the docking experiments of the TP-gold moiety into the truncated form of *Sm*TGR indicate a potential binding site for the molecule in Site 1 (Table 4 and Fig. 3). The best-docked conformation, i.e. the one with the lowest estimated free energy value, is located in this site. Here, TP-gold establishes hydrophobic interactions with the side chains of Pro572, Phe505 and Leu508, and the gold atom coordinates the nitrogen atom of His571 (distance 2.3 Å, Fig. 3). Noticeably, His571 is a key residue in the formation of a selenolate anion and has been found to be a catalytic residue in the human [18], *Plasmodium* [19] and *Sm*TGR homologues [20]. His571, Glu576 and Cys154 or Sec597 are conserved in the human, *Schistosomal* and *Plasmodium* enzymes, and form a catalytic triad, which, through the formation of a hydrogen bond network and a subsequent proton transfer, favors the formation and the stabilization of a thiolate in the redox site close to FAD and of a selenolate/thiolate at the C-terminal redox site, which are necessary for the oxido-reduction mechanism.

A likely interpretation of our results is that the interaction between the gold atom and His571 disrupts the catalytic triad, thus inhibiting the enzymatic activity. Notably, gold atom–histidine interactions have already been observed in gold compound–protein systems [21].

Experiments using the *Sm*TGRfl structure showed that, regardless of the presence of the tail, the compound binds in the same hydrophobic pocket (Site 1) as in the truncated protein with the same pattern of interactions (Fig. 4). Interestingly, in Site 1, TP-gold is oriented towards the C-terminal redox site and, in particular, it accommodates the gold moiety in proximity of Sec597.

Docking TP-gold into both the truncated and full-length *Sm*TGR variants devoided of the NADPH cofactor did not produce any solution, thus suggesting that a competitive binding with the cofactor does not occur.

3.4. P. falciparum Thioredoxin Reductase (PfTR)

3.4.1. PfTR homology model

As mentioned above, Auranofin is also known to inhibit *Plasmodium* and it is tempting to speculate that the target in the parasite is *Pf*TR, the enzyme homologous to SmTGR in the malaria causative agent.

The structure of *Pf*TR has not been experimentally determined, but it is possible to build a reliable homology model using the crystal structures of *Mm*TR, *Hs*TR, and *Sm*TGR (see Section 2). The model was built for the enzyme native dimeric form and includes the FAD cofactor (Fig. 1B).

As it can be appreciated from the target-template sequence alignment (Fig. S1), the *Pf*TR sequence contains a region of 35 residues located at the N-terminal end which is absent in the template sequences. According to the DISOPRED2 disorder predictor [22], this region is intrinsically disordered and was therefore not modeled. The highest degree of sequence similarity (~92%) is observed in the region corresponding to the catalytic site close to FAD (Site 1). In particular, the N-terminal hexapeptide CVNVGC, which contains two catalytic cysteines, Cys88 and Cys93, is strictly conserved, and so are the residues forming the FAD-binding cavity: Ser231, Tyr232, Val233, Ala313, Ile314, Gly315 and Arg316 (residues are numbered according to the *Pf*TR sequence). A lower degree of conservation occurs at the C-terminal redox center, where both the *Hs*TR and *Sm*TGR sequences have a cysteine and a selenocysteine in two adjacent positions, whereas the *Pf*TR sequence displays two cysteines (C535 and C540) separated by four residues.

The last ten C-terminal residues (Lys532-Gly541) are not present in the available crystal structures of the three templates, likely because of their flexibility, and the corresponding residues of *Pf*TR were not modeled. This implies that the C-terminal cysteine–cysteine pair is not included in the model.

The MetaMQAPII per-residue prediction accuracy score for the model is in the high accuracy range (Fig. S2, Supplementary Material). Additionally, the ProQ scores for the model quality estimate (MaxSub = 0.599 and LGscore = 6.930) indicate that the model is very reliable (MaxSub > 0.5 and LGscore > 5 correspond to good and very good model quality, respectively).

3.4.2. Docking experiments of AF and TP-gold into the PfTR model

Docking experiments of AF into the *Pf*TR model (which does not include the C-terminal tail) produced results similar to those obtained on the truncated form of *Sm*TGR: Solutions do not cluster in any specific region of the protein surface including Site1 and the NADPH pocket. Furthermore, all docked complexes have a high estimated binding free energy suggesting that a direct interaction between AF and *Pf*TR is unlikely (Tables 2 and 3).

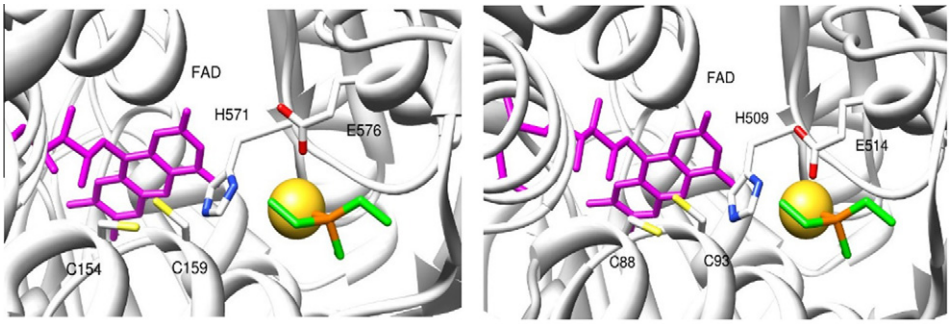

Fig. 3. The best docked conformation of TP-gold in truncated *Sm*TGR and *Pf*TR. FAD is in violet sticks. The gold atom is shown as a yellow sphere. Residues interacting with the gold atom are in sticks. (For interpretation of the references to color in this figure legend, the reader is referred to the web version of this article.)

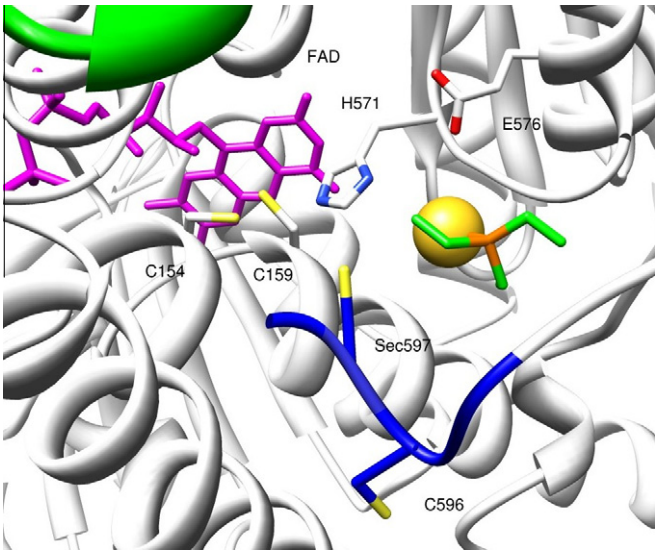

Fig. 4. The best docked conformation of TP-gold in full-length *Sm*TGR. FAD is in violet sticks. The gold atom is shown as a yellow sphere. Residues interacting with the gold atom are in sticks. The C-terminal tail of the protein is highlighted in blue. (For interpretation of the references to color in this figure legend, the reader is referred to the web version of this article.)

Conversely and interestingly, blind docking experiments of TP-gold into the *Pf*TR model show that the compound can bind in Site 1. Drug orientation and energy (Table 4) are very similar to those obtained for the corresponding site in the truncated *Sm*TGR: TP-gold lies in a hydrophobic region delimited by Pro510, Phe429 and Leu432. Additionally, it establishes hydrophobic interactions with the Asp512 backbone. The gold atom is coordinated in a linear geometry with one of the side chain nitrogens of His509 (distance 2.7 Å), which is essential for the enzymatic activity [19] (Fig. 3).

We refined the blind docking results in this interesting region using a smaller grid spacing (0.375 Å) and found binding modes essentially identical to those observed in the blind docking experiment (Table 4).

Neither AF nor TP-gold seem to be competing with NADPH; in fact only two high-energy AF poses have been observed in the NADPH binding site (estimated free energy: −1.25 kcal/mol) whereas no solutions for TP-gold are found in this site.

4. Discussion

In silico molecular docking is a powerful technique for structure-based drug design, which can be applied when the atomic coordinates of a protein of interest are available or can be reliably modeled. We exploited this tool to investigate and understand the mode of action of an interesting inhibitor compound of *S. mansoni*, Auranofin (AF), known to interact with the parasite Thioredoxin Glutathione Reductase and assessed whether the molecule and/or its triethylphosphine-gold (TP-gold) derivative are able to tightly bind to the enzyme or whether one or both of them can only form transient interactions with the protein to transfer the gold atoms to its reactive sites.

Our results show that it is extremely unlikely that the whole AF molecule can bind to the enzyme and that the most plausible mechanism for the gold transfer reaction in *Sm*TGR involves initial binding to the Sec followed by an intra-molecular transfer to Cys596, in agreement with the hypothesis of some authors [12]. In addition, our data indicate that both binding and transient interactions of TP-gold are possible and likely.

We also exploited molecular modeling techniques and docking experiments to evaluate the likelihood that the observed inhibitory action of AF on *Plasmodium* can target the homologous enzyme (*Pf*TR) and be exerted through a similar mechanism. Also in this case, the whole AF molecule is not expected to establish other than a transient interaction with the enzyme, while TP-gold might either interact transiently or form a complex with the enzyme. Importantly, the putative binding sites of TP-gold on the *Plasmodium* and *Schistosomal* enzymes are located in equivalent positions and establish very similar patterns of interactions.

Our computational studies and docking experiments were possible thanks to the availability of the crystal structure of both the truncated and full-length versions of *Sm*TGR. This allowed us, on one hand, to carry out docking studies in diverse structural conditions and, on the other, to build a reliable three-dimensional model for *Pf*TR. Furthermore, previous biochemical studies [12] helped us gaining confidence in our results.

The observation that TP-gold can potentially bind to the proteins is of high relevance since the putative existence of a non transient interaction opens the road to further studies for improving both the affinity and the specificity of the molecule and, given the high relevance of both parasites for human health, we hope that such a route will be pursued in the future by academic or industrial pharmaceutical chemical laboratories.

Acknowledgments

We thank the members of the Fondazione Roma Research Unit led by Prof. Maurizio Brunori for useful discussions and Prof. Arthur Lesk for critically reading the manuscript. This work was partially supported by Award number KUK-I1-012-43 made by King Abdullah University of Science and Technology (KAUST), FIRB Proteomica, Ministery of Health Grant Contract No. Onc_Ord 25/07, Fondazione Roma and the IIT SEED project.

Appendix A. Supplementary data

Supplementary data associated with this article can be found, in the online version, at doi:10.1016/j.bbrc.2011.12.009.

References

[1] E.A. Winzeler, Malaria research in the post-genomic era, Nature 455 (2008) 751–756.
[2] D.A. Fidock, Drug discovery: priming the antimalarial pipeline, Nature 465 (2011) 297–298.
[3] F.J. Gamo, L.M. Sanz, J. Vidal, et al., Thousands of chemical starting points for antimalarial lead identification, Nature 465 (2010) 305–310.
[4] A.N. Kuntz, E. Davioud-Charvet, A.A. Sayed, et al., Thioredoxin glutathione reductase from *Schistosoma mansoni*: an essential parasite enzyme and a key drug target, PLoS Med. 4 (2007) e206.
[5] F. Angelucci, A.E. Miele, G. Boumis, et al., Glutathione reductase and thioredoxin reductase at the crossroad: the structure of *Schistosoma mansoni* thioredoxin glutathione reductase, Proteins 72 (2008) 936–945.
[6] F. Angelucci, D. Dimastrogiovanni, G. Boumis, et al., Mapping the catalytic cycle of Schistosoma mansoni thioredoxin glutathione reductase by X-ray crystallography, J. Biol. Chem 285 (2010) 32557–32567.
[7] Z. Krnajski, T.W. Gilberger, R.D. Walter, et al., Thioredoxin reductase is essential for the survival of *Plasmodium falciparum* erythrocytic stages, J. Biol. Chem. 277 (2002) 25970–25975.
[8] A.R. Sannella, A. Casini, C. Gabbiani, et al., New uses for old drugs Auranofin, a clinically established antiarthritic metallodrug, exhibits potent antimalarial effects in vitro: Mechanistic and pharmacological implications, FEBS Lett. 582 (2008) 844–847.
[9] K.P. Bhabak, B.J. Bhuyan, G. Mugesh, Bioinorganic and medicinal chemistry: aspects of gold(I)–protein complexes, Dalton Trans 40 (2011) 2099–2111.
[10] S.S. Gunatilleke, C.A. de Oliveira, J.A. McCammon, et al., Inhibition of cathepsin B by Au(I) complexes: a kinetic and computational study, J. Biol. Inorg. Chem. 13 (2008) 555–561.
[11] H.M. Berman, J. Westbrook, Z. Feng, et al., The protein data bank, Nucleic Acids Res. 28 (2000) 235–242.
[12] F. Angelucci, A.A. Sayed, D.L. Williams, et al., Inhibition of *Schistosoma mansoni* thioredoxin-glutathione reductase by auranofin: structural and kinetic aspects, J. Biol. Chem. 284 (2009) 28977–28985.
[13] A. Sali, T.L. Blundell, Comparative protein modelling by satisfaction of spatial restraints, J. Mol. Biol. 234 (1993) 779–815.
[14] B. Wallner, A. Elofsson, Identification of correct regions in protein models using structural alignment, and consensus information, Protein Sci. 15 (2006) 900–913.
[15] M. Pawlowski, M.J. Gajda, R. Matlak, et al., MetaMQAP: a meta-server for the quality assessment of protein models, BMC Bioinformatics 9 (2008) 403.
[16] G.M. Morris, R. Huey, W. Lindstrom, et al., AutoDock4 and AutoDockTools4: automated docking with selective receptor flexibility, J. Comput. Chem. 30 (2009) 2785–2791.
[17] F. Zsila, Z. Bikadi, E. Hazai, et al., Organogold complexes probe a large beta-barrel cavity for human serum alpha1-acid glycoprotein, Biochim. Biophys. Acta 1784 (2008) 1106–1114.
[18] W. Brandt, L.A. Wessjohann, The functional role of selenocysteine (Sec) in the catalysis mechanism of large thioredoxin reductases: proposition of a swapping catalytic triad including a Sec-His-Glu state, Chembiochem 6 (2005) 386–394.
[19] T.W. Gilberger, R.D. Walter, S. Muller, Identification and characterization of the functional amino acids at the active site of the large thioredoxin reductase from *Plasmodium falciparum*, J. Biol. Chem. 272 (1997) 29584–29589.
[20] H.H. Huang, L. Day, C.L. Cass, et al., Investigations of the catalytic mechanism of thioredoxin glutathione reductase from Schistosoma mansoni, Biochemistry 50 (2011) 5870–5882.
[21] J. Zou, P. Taylor, J. Dornan, et al., First crystal structure of a medicinally relevant gold protein complex: unexpected binding of, Angew. Chem. Int. Ed. 39 (2000) 2931–2934.
[22] J.J. Ward, J.S. Sodhi, L.J. McGuffin, et al., Prediction and functional analysis of native disorder in proteins from the three kingdoms of life, J. Mol. Biol. 337 (2004) 635–645.